

CRCLEME

Cooperative Research Centre for
Landscape Evolution & Mineral Exploration



CSIRO
EXPLORATION
AND MINING



Australian Mineral Industries Research Association Limited ACN 004 448 266



**OPEN FILE
REPORT
SERIES**

RADIOELEMENTS IN WEATHERED SHALES AND MAFIC VOLCANICS, PANGLO GOLD DEPOSIT, EASTERN GOLDFIELDS, WESTERN AUSTRALIA

K.M. Scott and B.L. Dickson

CRC LEME OPEN FILE REPORT 71

February 1999

(CSIRO Division of Exploration Geoscience Report 41R, 1989.
Second impression 1999)

CRC LEME is an unincorporated joint venture between The Australian National University, University of Canberra, Australian Geological Survey Organisation and CSIRO Exploration and Mining, established and supported under the Australian Government's Cooperative Research Centres Program.



RADIOELEMENTS IN WEATHERED SHALES AND MAFIC VOLCANICS, PANGLO GOLD DEPOSIT, EASTERN GOLDFIELDS, WESTERN AUSTRALIA

K.M. Scott and B.L. Dickson

CRC LEME OPEN FILE REPORT 71

February 1999

(CSIRO Division of Exploration Geoscience Report 41R, 1989.
Second impression 1999)

© CSIRO 1989

RESEARCH ARISING FROM CSIRO/AMIRA REGOLITH GEOCHEMISTRY PROJECTS 1987-1993

In 1987, CSIRO commenced a series of multi-client research projects in regolith geology and geochemistry which were sponsored by companies in the Australian mining industry, through the Australian Mineral Industries Research Association Limited (AMIRA). The initial research program, "Exploration for concealed gold deposits, Yilgarn Block, Western Australia" (1987-1993) had the aim of developing improved geological, geochemical and geophysical methods for mineral exploration that would facilitate the location of blind, buried or deeply weathered gold deposits. The program included the following projects:

P240: Laterite geochemistry for detecting concealed mineral deposits (1987-1991). Leader: Dr R.E. Smith.
Its scope was development of methods for sampling and interpretation of multi-element laterite geochemistry data and application of multi-element techniques to gold and polymetallic mineral exploration in weathered terrain. The project emphasised viewing laterite geochemical dispersion patterns in their regolith-landform context at local and district scales. It was supported by 30 companies.

P241: Gold and associated elements in the regolith - dispersion processes and implications for exploration (1987-1991). Leader: Dr C.R.M. Butt.

The project investigated the distribution of ore and indicator elements in the regolith. It included studies of the mineralogical and geochemical characteristics of weathered ore deposits and wall rocks, and the chemical controls on element dispersion and concentration during regolith evolution. This was to increase the effectiveness of geochemical exploration in weathered terrain through improved understanding of weathering processes. It was supported by 26 companies.

These projects represented "an opportunity for the mineral industry to participate in a multi-disciplinary program of geoscience research aimed at developing new geological, geochemical and geophysical methods for exploration in deeply weathered Archaean terrains". This initiative recognised the unique opportunities, created by exploration and open-cut mining, to conduct detailed studies of the weathered zone, with particular emphasis on the near-surface expression of gold mineralisation. The skills of existing and specially recruited research staff from the Floreat Park and North Ryde laboratories (of the then Divisions of Minerals and Geochemistry, and Mineral Physics and Mineralogy, subsequently Exploration Geoscience and later Exploration and Mining) were integrated to form a task force with expertise in geology, mineralogy, geochemistry and geophysics. Several staff participated in more than one project. Following completion of the original projects, two continuation projects were developed.

P240A: Geochemical exploration in complex lateritic environments of the Yilgarn Craton, Western Australia (1991-1993). Leaders: Drs R.E. Smith and R.R. Anand.

The approach of viewing geochemical dispersion within a well-controlled and well-understood regolith-landform and bedrock framework at detailed and district scales continued. In this extension, focus was particularly on areas of transported cover and on more complex lateritic environments typified by the Kalgoorlie regional study. This was supported by 17 companies.

P241A: Gold and associated elements in the regolith - dispersion processes and implications for exploration. Leader: Dr. C.R.M. Butt.

The significance of gold mobilisation under present-day conditions, particularly the important relationship with pedogenic carbonate, was investigated further. In addition, attention was focussed on the recognition of primary lithologies from their weathered equivalents. This project was supported by 14 companies.

Although the confidentiality periods of the research reports have expired, the last in December 1994, they have not been made public until now. Publishing the reports through the CRC LEME Report Series is seen as an appropriate means of doing this. By making available the results of the research and the authors' interpretations, it is hoped that the reports will provide source data for future research and be useful for teaching. CRC LEME acknowledges the Australian Mineral Industries Research Association and CSIRO Division of Exploration and Mining for authorisation to publish these reports. It is intended that publication of the reports will be a substantial additional factor in transferring technology to aid the Australian Mineral Industry.

This report (CRC LEME Open File Report 71) is a Second impression (second printing) of CSIRO, Division of Exploration Geoscience Restricted Report 41R, first issued in 1989, which formed part of the CSIRO/AMIRA Projects P241 and P263.

Copies of this publication can be obtained from:

The Publication Officer, c/- CRC LEME, CSIRO Exploration and Mining, PMB, Wembley, WA 6014, Australia. Information on other publications in this series may be obtained from the above or from <http://leme.anu.edu.au/>

Cataloguing-in-Publication:

Scott, K.M.

Radioelements in weathered shales and mafic volcanics, Panglo Gold Deposit, Eastern Goldfields, WA

ISBN 0 642 28275 7

1. Geochemistry - Western Australia 2. Volcanic ash, tuff, etc - analysis 3. Rocks, igneous - analysis.

I. Dickson, B.L. II. Title

CRC LEME Open File Report 71.

ISSN 1329-4768

PREFACE

The CSIRO-AMIRA project "Exploration for Concealed Gold Deposits, Yilgarn Block, Western Australia" has as its overall aim the development of improved geological, geochemical and geophysical methods for mineral exploration that will facilitate the location of blind, concealed or deeply weathered gold deposits. Module 2 of this project (P241) "Gold and Associated Elements in the Regolith - Dispersion Processes and Implications for Exploration" specifically aims inter alia

- (i) To determine characteristics useful for exploration, especially in areas of transported overburden for: a) further lateritic and supergene deposits, and b) primary mineralization - including that with no expression as appreciable secondary mineralization, and
- (ii) To increase knowledge of the properties and genesis of the regolith.

The CSIRO-AMIRA project (P263) "Improving the interpretation of airborne gamma ray surveys" aims to study the relationship of the radioelements in fresh and weathered rocks and soils.

Because of the desire to integrate research, similarity of objectives and almost complete overlap of sponsors of P263 with those of P241, this report is being distributed to both projects.

In particular this report (a) documents the abundances of radiometric elements present in several different rock types in the Eastern Goldfields, (b) uses the radiometric data with other geochemical and mineralogical data to propose a model for the weathering processes at Panglo, and (c) evaluates the potential usefulness of radiometric surveys for rock-type identification.

TABLE OF CONTENTS

	Page
SUMMARY	1
1. INTRODUCTION	2
2. SAMPLES	2
3. ANALYTICAL METHODS	3
4. DATA QUALITY	4
5. RESULTS	5
5.1 Weathered Mafic Volcanics (PSRC 230, 231)	5
5.2 Unweathered Volcanics and Dolerites (PSRCD 232, 306, 309)	6
5.3 Weathered Shales (PSRC 111, 340, 341, 342)	6
5.4 Unweathered Shales (PSRCD 309, 310)	7
5.5 Soils and Pisoliths	7
6. DISCUSSION	8
7. CONCLUSIONS	12
8. RECOMMENDATIONS FOR FUTURE WORK	13
9. ACKNOWLEDGEMENTS	13
10. REFERENCES	14

LIST OF TABLES

Table 1:	Radioelement abundances for Panglo drill hole profiles.
Table 2:	Recount data for volcanics and shales, Panglo.
Table 3:	Comparison of U and Th measured by delayed neutron counting and XRF respectively, with gamma-spectrometry derived eU and eTh for 13 samples of weathered shales from PSRC 340.
Table 4:	Average abundances of radioelements in weathered shales from four drill holes, Panglo.
Table 5:	Radioelement concentrations in soils at Panglo.
Table 6:	Radioelement concentrations and Fe phases in pisoliths from soils at Panglo.
Table 7:	Selected chemical data from mineralized and barren holes through shale at Panglo.

LIST OF FIGURES

- Fig 1: Location of reverse circulation drill holes sampled for this study (after mapping by Pancontinental Mining Ltd.)
- Fig 2: Decay series of ^{238}U and ^{232}Th with major gamma emitting radionuclides highlighted to show their occurrence late in both series.
- Fig 3: Radioelement and mineralogical profile through the mineralized hole PSRC 111.
- Fig 4: Radioelement and mineralogical profile through the mineralized hole PSRC 341.
- Fig 5: Radioelement and mineralogical profile through the mineralized hole PSRC 342.
- Fig 6: Radioelement and mineralogical profile through the barren hole PSRC 340.
- Fig 7: Profile of radioelements (K, eU and eTh) and the elements (Au, Ba, Ca, Ce, Fe and Sr) through the mineralized hole PSRC 342.
- Fig 8: Profile of radioelements (K, eU and eTh) and the elements (Au, Ba, Ca, Ce, Fe and Sr) through the barren hole PSRC 340.

SUMMARY

The K, eU and eTh contents of 111 samples of shales, mafic volcanics and dolerites from the Panglo gold deposit have been determined radiometrically. Shales have consistently higher K, eU and eTh contents than the mafic volcanics and dolerites. However, within shale profiles above the Au mineralization, eTh and eU contents are low relative to equivalent barren profiles. This feature is similar to the behaviour of Sr in the same shale profiles (Scott, 1989a) and, with the additional constraints imposed by the geochemistry of Th, an hypothesis to account for the mineralogical and geochemical features in the shale is presented. Under the acid sulfate conditions resulting from the weathering of sulfides, Th (and U) are envisaged as having migrated from more acid areas to what is now the periphery of the deposit where they are adsorbed onto and/or incorporated into Fe oxides. Strontium in hanging wall rocks at the edge of the deposit is contained largely in Na-rich phyllosilicates which formed during the interaction of later saline groundwaters with the original mica. This saline ground water is probably responsible for the formation of the Ag-free supergene gold deposit at Panglo.

Twenty-seven soil samples from over the deposit have similar concentrations of K, eU and eTh. Because they show no variations which can be related to the underlying lithology, a major transported component within the soils is suggested. The eU and eTh contents of pisoliths within the soils indicate that eU and eTh are specifically related to the iron oxide components.

1. INTRODUCTION

The three naturally occurring radioactive elements potassium, uranium and thorium occur in varying amounts in rock-forming minerals and can often be used to distinguish different rock types. In addition, the three elements have diverse chemistries: K being readily soluble but commonly incorporated into or adsorbed onto clays; U being soluble only under oxidizing conditions but easily adsorbed onto iron oxides; Th being soluble only under highly acid conditions. Thus, alteration and weathering may result in relative changes in concentration of the three elements.

This report details potassium, uranium and thorium abundances measured by gamma-ray spectrometry in samples from the Panglo gold deposit, 30 km NNW of Kalgoorlie. Gold at Panglo occurs as a blanket of supergene mineralization at a depth of 35 - 40 m hosted by weathered shales and mafic volcanics by a shear zone.

Samples were selected from the different zones within the weathered profile identified by Scott (1989a,b) to determine how the radioelements abundances varied during weathering of shales and mafic volcanics in the Eastern Goldfields region of the Yilgarn Block. Soils were also analyzed to determine whether features in the weathered rocks would be discernible in surface or airborne gamma-ray surveys.

2. SAMPLES

A total of 96 weathered samples were selected from reverse circulation drill holes penetrating mafic volcanics (PSRC 230, 231), one through shales with sub-economic Au mineralization (PSRC 340 - denoted as a "barren" hole) and three through shales intersecting economic Au mineralization (PSRC 111, 341 and 342). All of these drill holes occur along the line 4200N (Fig. 1). Two partially weathered samples of dolerite from a location 1.3km to the north and various samples of unweathered volcanics, dolerite and shale from diamond drilling were also analyzed. All drill holes were inclined at 60° to the east and in subsequent discussion distances down these holes are referenced rather than the actual depth below the surface.

The top 5 - 6 cm of soil from 27 locations mainly along line 4200N but including pisolith-rich material from the eastern edge of the prospect, north and south of that line, were collected and analyzed. Pisoliths from several of the soil samples were also analyzed separately when approximately 50 g of such material could be obtained.

3. ANALYTICAL METHODS

The samples were analyzed using gamma-ray spectrometry to measure potassium (K), gamma-equivalent uranium (eU) and gamma-equivalent thorium (eTh). Gamma rays emitted when ^{40}K decays to ^{40}Ar directly indicate K contents. However, the gamma radiation emitted during the decay of U and Th comes principally from daughters ^{214}Pb and ^{214}Bi for U and ^{208}Tl for Th (all of which occur late in the respective decay series as shown in Fig 2). Thus gamma radiation is not a direct measure of either U or Th, but rather is a measure of the preceding long-lived radium isotope in each decay series (^{226}Ra in the U series and ^{228}Ra in the Th series). The measurement of U and Th by their daughter radionuclides is therefore identified by the terminology "gamma-equivalent" (i.e. eU and eTh). The different chemistries of U, Th and Ra can lead to separation of the three elements as a result of weathering or alteration and "gamma-equivalent" results can be greater than or less than the chemical U or Th content of a sample.

The measurements were made by sealing 50g of crushed sample in a 50 ml metal can and, after a delay of at least 30 days, recording the gamma-ray energy spectra of each sample with a shielded gamma-ray spectrometer in the laboratory. The delay enables radon (^{222}Rn), which may be lost during sample crushing and drying, to re-establish equilibrium with its parent ^{226}Ra . Full 256 channel spectra were recorded and processed by a matrix inversion technique that also corrects for any gain drift in the spectrometer. Standards for calibrating the analysis were potassium sulfate, and two internationally cross-calibrated concretes doped with U and Th.

4. DATA QUALITY

The results of the analyses (Table 1) show that the volcanics are generally low in both eU and eTh and occasionally low in K whereas the shale samples have much higher concentrations of all three radioelements. The low concentrations in the volcanics present an analytical problem as these levels are at or below the statistically determined detection limits for the 50g sample size used here. This is shown by the uncertainty given for eU and eTh in Table 1 (approximately 0.4 and 1.0 ppm respectively). This uncertainty includes contributions from both the sample and standard counts and uncertainty in the assigned values of the standard analyses. These errors are fully propagated in the calculation and least squares estimation of the concentrations.

Repeat analyses were made of seven samples to investigate actual uncertainty. The results (Table 2) show that for potassium in the volcanics and the three radioelements in the shale samples, repeatability is much better than indicated by the standard deviations of the individual measurements, i.e. the statistical method of assessing the standard deviation appears to overestimate uncertainty. For eU and eTh in the volcanics, estimation of standard deviation is similar to the scatter in the results which are close to the limit of detection.

Samples from four of the drill holes had been previously analyzed for K by X-ray fluorescence spectrometry (Scott, 1989a,b). The agreement between the radiometric and chemical potassium is very good, with the average difference, expressed as a percentage of the chemically determined K, being normally distributed about zero. Although K results have been previously reported, they are discussed below for the sake of completeness of the radiometric determinations.

Thirteen samples from PSRC 340 were analyzed for U by T. Wall (Australian Nuclear Science and Technology Organization, Lucas Heights, Sydney) using delayed fission neutron counting to obtain an indication of the accuracy of the eU measurements and to determine whether there is U - Ra disequilibrium in the weathered shales. The uncertainty in the U values is approximately 0.10 ppm whereas the uncertainty in the eU values is higher, at approximately

0.5 ppm. The disequilibrium ratios (chemical U / gamma U) (Table 3) show that samples above 33 m tend to have $U > eU$ whereas deeper samples have $U < eU$. If this trend is significant it may reflect either the result of mobilization of Ra from the more weathered surface samples to deeper in the profile or transport of U towards the surface. However, at the U concentrations being considered, eU approximates to total U. In addition, these samples were analyzed for Th in the North Ryde laboratories of CSIRO, Division of Exploration Geoscience, using X-ray fluorescence spectrometry (XRF). This method has a detection limit of 5 ppm and the accuracy of values at twice the detection limit is uncertain. The XRF-derived Th values tend to be higher than the eTh values (Table 3) but, considering the uncertainty associated with the XRF values, not significantly so.

5. RESULTS

5.1 Weathered Mafic Volcanics (PSRC 230, 231)

1) Potassium in the volcanic profile varies between <0.1 and 2.2% (Table 1) and reflects the abundances of muscovite in samples (Scott 1989b). The distribution of K within the weathered mafic volcanics is normal with a mean of 0.75% (s.d. 0.66). No variation with depth has been found.

2) Gamma-uranium shows two populations; 5 of the 8 samples from within the top 7 m of the two holes have higher eU contents (1.8 ± 0.3 ppm eU) than the other 26 samples which are normally distributed about a mean of 0.40 ppm (s.d. 0.25, median 0.43 ppm). This latter value probably represents the best estimate for the concentration of eU in the weathered volcanics.

3) Concentrations of eTh in the volcanics are generally low, having a normal distribution about 0.1 ppm (s.d. 0.9) which is not statistically different from zero.

4) Two samples of partially weathered dolerite from PSRC 151 have low abundances of all three radioelements.

5.2 Unweathered Volcanics and Dolerites (PSRCD 232, 306, 309)

Potassium contents in the unweathered volcanics and dolerites vary between zero and 1.3%, directly reflecting muscovite abundances (as above). Gamma-uranium and -thorium are both low with only one analysis of each having a statistically significant value. Thus the average abundances at Panglo are lower than those for Australian Archaean mafic volcanics, i.e. 0.3% K, 0.2 ppm U and 0.8 ppm Th (Taylor and McClennan, 1985).

5.3 Weathered Shales (PSRC 111, 340, 341, 342)

Radioelement concentrations in the four shale profiles are individually summarized in Table 4 and diagrammatically displayed in Figs 3 - 6.

- 1) Potassium in the shales is normally distributed about 2.1 % (s.d. 0.65, median 2.0). Some particularly high values occur close to the surface of PSRC 342 and between 14 and 21 m in PSRC 111. These two holes also show a trend of decreasing K with depth (Table 1; Figs 3 and 5).
- 2) Gamma-uranium contents in the shales are distributed about 1.5 ppm but significant variations are seen between and within the four drill holes. High values occur in PSRC 340 at 42 and 59 m, in PSRC 342 at 41 m, in PSRC 111 at 35 m and in PSRC 341 at 53 m (Table 1). The barren hole (PSRC 340) also tends to have more eU than the other holes (Table 4) and to show some tendency for eU to increase with depth. Hole PSRC 111 has a significantly lower average eU content than the other mineralized holes.
- 3) Gamma-thorium contents in the four holes in shale show significant variations (Figs 3 - 6). In the mineralized holes (PSRC 111, 341 and 342), eTh contents in the top 40 m are generally below 8 ppm but are greater than 10 ppm in the corresponding interval in the barren hole (PSRC 340). The holes PSRC 342 and 341 show higher values (>10 ppm) associated with mineralization and for some metres below but the mineralized interval in PSRC 111 is characterised by low eTh contents. Th contents below 45 m are lower than in the top 40 m of each hole except in PSRC 341 where higher values associated with the mineralization are retained to the bottom of that hole.

5.4 Unweathered Shales (PSRCD 309, 310)

Radioelements were analyzed in six samples of unweathered dolomitic and carbonaceous shale. Potassium varies between 1 and 3 %, depending upon how much muscovite is present, eU contents vary about 1 ppm and eTh contents are between 4 and 6 ppm (Table 1). Thus, the values measured in weathered material at the base of most of the sampled profiles (section 5.3) are similar to those of the unweathered material.

5.5 Soils and Pisoliths

The 22 samples of soil collected from along the line 4200N have very similar radioelement concentrations. The K content has a mean value of 0.60 %, (s.d 0.14), eU a mean value of 2.0 ppm (s.d 0.4) and eTh a mean value of 6.0 ppm (s.d 0.8) (Table 5). However, there is some tendency for K to decrease and eU to increase towards the west.

Sample 108102 from line 4200N was almost entirely pisolitic. This was separated into four fractions by first sieving into coarse (+1.7 mm) and fine (-1.7 mm) subsamples and then by density differentiation in a heavy liquid (methylene iodide: S.G. = 3.2) into "floats" and "sinks". All four fractions have little K but the eU and eTh concentrations vary significantly from the very low contents of the fine float fraction to the high contents of the fine sink fraction. Samples 108104 and 108113 also contained sufficient pisoliths to analyze separately. These show reduced K relative to their host soil, elevated eU but similar eTh contents. The pisoliths from sample 108104 are more goethitic than many of the others and do not contain maghemite (Table 6).

Five other soil samples from north and south of the 4200N line were collected. Two of these (samples 108077 and 108119) have lower K and higher eU and eTh than the other soils. Pisoliths in these two samples were separated and analyzed. The hematite- and maghemite-rich pisoliths have similar eU, higher eTh and much lower K contents than their host soil (c.f. Tables 5 and 6).

The slight tendency for the soils from along the line 4200N to decrease in K and increase in eU and eTh towards the west where the underlying rocks are volcanics rather than sediments is at variance with the observed lithological associations developed at Panglo. Thus, the soils do not appear to be related to the underlying rocks. Indeed aerial photographs of the area clearly indicate the presence of sheetwash over this part of the deposit. However, because the soil is usually thin (< 0.5 m), it generally comprises less than half of the initial metre of reverse circulation drill cuttings and radioelement determinations on such composite samples are not seriously affected by the soil (Table 1).

6. DISCUSSION

Potassium can be largely related to the presence of muscovite within individual samples. Thus, the more micaceous zones within the weathered profiles can be readily identified by radiometric K determinations (Table 1). With the greater abundance of such mica in unweathered shales than in unweathered volcanics and its degree of resistance to weathering, greater muscovite and hence higher K contents are present in the weathered shales.

Within the volcanics eU and eTh abundances are close to the limit of detection of the radiometric method employed so their significance cannot be assessed. Although eU and eTh are generally more abundant in the profiles through shales than through volcanics, their distributions are complex and their presence cannot be easily assigned to specific mineralogical hosts. Accessory minerals such as monazite, xenotime, thorite-uranite, thorianite-uraninite, allanite and zircon may all contain percentage amounts of one or both of uranium and thorium (Rodgers and Adams, 1974). One of these potential major sources, a monazite grain, was identified in the shale sample 108074 but that grain contained < 0.5 % Th (Scott, unpublished data). Furthermore, some alpha-track recordings made on thin sections of two fresh shale samples from PSRCD 309 showed no evidence for eU or eTh rich mineral grains. The recorded tracks were uniformly distributed across the section indicating broad dispersion of both eU and eTh through the rock-forming minerals in the shale.

In the shale, weathering in the top 40 m in the unmineralized profile (PSRC 340) results in eTh contents more than double the 5 ppm found in the fresh shales (Table 1, Fig 6). This indicates that the weathered shales have been enriched in eTh during weathering. Mineralized profiles show eTh and eU depletions close to the surface although higher eTh (and eU) may occur associated with mineralization and for some metres below as in holes PSRC 342 and 341. The low Th contents of resistant minerals (seen above) suggest that such distributions cannot be readily explained by simple residual concentration of resistate accessory Th (and U) phases, instead chemical mobility during weathering appears to have occurred. The association of eU and eTh with iron oxides seen in the pisoliths (Table 6) could also imply chemical mobility of both radioelements during weathering.

The distributions of eU and eTh in PSRC 340 and 342 were compared to those of Au, Ba, Fe, Sr (previously reported: Scott, 1989a) and Ce (new data, obtained by XRF) and Ca (new data, obtained by ICP-AES) (Table 7).

These elements were selected because:

1. Ba forms insoluble sulfates which are excellent hosts for radium (the long-life daughter of U which actually determines the gamma ray emission measured as eU, Fig 2);
2. Ca often behaves in a geochemically similar manner to Sr;
3. Ce often behaves in a geochemically similar manner to Th.
4. Fe, as indicated by the measurements on the pisoliths, can concentrate U and Th;
5. low Sr contents through the profile above mineralization and high levels lateral to mineralization are possibly related to the mineralization (Scott, 1989a).

Profiles of the various elements down PSRC 342 (Fig 7) indicate that:-

Au is associated with high eU, eTh and Fe.

Ba is related to K but not eU.

Ca is unrelated to Sr.

Ce is associated with eTh especially at about 40 m.

Fe is elevated at ~ 40 m where eU and eTh are also elevated but eU and eTh are not present in the high Fe zone at the top of the hole.

Sr increases with depth to ~ 40 m like eTh but, whereas eTh has a maximum there, Sr has a minimum.

Profiles down PSRC 340 (Fig 8) indicate that:-

Au is developed just above the highest Fe, eU and eTh samples.

Ba has its highest abundances in the top few metres of this hole but then essentially follows the distribution of K. It shows no relationship to eU.

Ca is unrelated to Sr.

Ce like eTh shows a general decrease down the hole.

Fe is most abundant at ~ 42 m where eU and eTh attain their maximum development.

Sr is unrelated to any of the radioelements in PSRC 340.

In summary - Au shows some association with eU and, more particularly, eTh at approximately 40 m down both drill holes.

- Ba is strongly associated with K, but not with eU.
- Ca and Sr are unrelated i.e. Sr does not reflect carbonate abundances. Neither element is related to a radioelement.
- Ce behaves in a similar manner to eTh, especially above the ore horizon.
- Fe shows a general elevation at about 40 m where eU, eTh and Au are also enriched.

The behaviour of Ba and Ca is not considered further but constraints imposed by the behaviour of the other elements at Panglo can be used to construct a model for the weathering.

Thorium has only one oxidation state, Th(IV) which is generally very insoluble except in acid sulfate solutions (Langmuir and Herman, 1980).

Cerium has two oxidation states; Ce(III) under most conditions and Ce(IV) in

very oxidising conditions such as in modern oceans (e.g. Goldberg, 1954). In the IV state Ce behaves in a similar manner to Th(IV), possibly explaining the association of Ce and eTh in the two holes. Thus, it can be postulated that under oxidising acid sulfate conditions developed during pyrite weathering, Th and Ce have been mobilized from the most acidic areas (PSRC 342), and precipitated in lateral, less acidic environments (PSRC 340).

Uranium has two oxidation states, U(IV) under reducing conditions where it is immobile and U(VI) in oxidising conditions where it can form stable complexes and be mobilized (Langmuir, 1978). However, U(VI) is highly adsorbed onto amorphous iron oxides/hydroxides at pH 5 to 8 in the absence of complexing anions (Hsi and Langmuir, 1985) and this can limit its mobility. At Panglo higher U abundances present lateral to the ore (i.e. PSRC 340; Table 4) suggest that U may have moved from the acid oxidising environment of the mineralized profiles as U(VI) and under less acid conditions become associated with Fe (as seen above) by adsorption onto and/or incorporation into ferric oxides/hydroxides. The presence of high (>2000 ppm) As in such ferruginous phases at this location (Scott, unpublished data) is also consistent with such a process.

The mobility of Sr is hindered by the presence of sulfates and is most soluble in strongly reducing solutions where SO_4 concentrations are low. Strontium occurs in the weathered shale mainly within Na-rich mica and illite (paragonite and brammallite respectively) at levels >500 ppm (Scott, unpublished data). As the more K-rich micas from the unweathered shales contain less than 100 ppm Sr (Scott, unpublished data), Sr appears to be incorporated into the Na-rich phyllosilicates during the interaction of saline groundwaters with original muscovite.

Thus the distribution of Sr probably reflects changes which occurred during an arid weathering stage at Panglo. Such saline conditions are not related to the acid sulfate conditions that led to the formation of alunite (and mobilized Ce, U and Th). These two stages of weathering could account for the lack of correlation between Sr and the other trace elements. Furthermore, the occurrence of high eTh contents with mineralization in PSRC 341 and 342 but not in PSRC 111 implies that the mineralization is not specifically related to acidity. In fact, the Ag-free nature of the gold grains studied under the scanning electron microscope (Scott, unpublished data) suggests that it was

probably transported and precipitated by saline groundwaters (cf. Mann, 1984). Nevertheless, the association of eTh and gold in some profiles does suggest that in situ analysis of eTh during pit mapping has potential as a guide to gold mineralization.

7. CONCLUSIONS

Weathered shales can be distinguished from weathered mafic volcanics on the basis of their higher K, eU and eTh contents. Weathered shales above mineralization at Panglo have lower eTh (and eU) content than laterally equivalent shales from barren profiles. However elevated eTh contents may be associated with the Au mineralization in mineralized profiles. By considering the distributions of eU, eTh, Ce, Sr, and Fe it appears that the heavy elements U, Th and Ce were mobilized from the zone of most intense acid development above where Au mineralization now exists. These metals were then precipitated lateral to this zone in a less acid environment. A later introduction of saline groundwaters mobilized Sr and possibly led to the formation of the Au mineralization.

Soils over the prospect have relatively uniform K, eU and eTh contents, suggesting a major transported component within them. Thus surface (or airborne) radiometric survey of the prospect would not have differentiated the various lithologies at Panglo nor have shown the negative eTh (and U) anomalies above the shale-hosted mineralization. Nevertheless variable eTh contents within weathered shales do suggest that in situ radiometric determinations during pit mapping may have potential as a guide to ore.

8. RECOMMENDATIONS FOR FUTURE WORK

Further work is recommended to confirm the trends observed above.

1) Samples from a hole within shale more remote from the mineralization along the line 4200N should be examined to determine whether the elevated concentrations of Sr, Ce and eTh in the PSRC 340 do indicate an extended halo around the Panglo mineralization.

2) Samples from drill holes intermediate between PSRC 340 and 342 should be analysed for the trace elements identified in this study as being significant indicators of the geochemical processes that have occurred at Panglo.

3) Additional samples of mineralization should be analyzed to determine the significance of the spot high eTh and eU contents with mineralization in PSRC 342.

9. ACKNOWLEDGEMENTS

The management of the Exploration Division of Pancontinental Mining Ltd. (especially Doug Currie) is thanked for a willingness to provide pulped samples, logs and plans of the Panglo deposit. In particular the ready assistance of Bob Howard (Project Geologist - Panglo) in advising of the best sections to sample and organizing that sampling is acknowledged.

A. Sheehan assisted with radiometric determinations and the additional XRF analyses were performed by A. Martinez, both from the North Ryde laboratories of the CSIRO Division of Exploration Geoscience.

10. REFERENCES

- Goldberg, E.D., 1954. Marine geochemistry, 1. Chemical scavengers of the sea. *J. Geol.*, 62, 249-265.
- Hsi, C.D. and Langmuir, D., 1985. Adsorption of uranyl onto ferric oxyhydroxides: Application of the surface complexation site-binding model. *Geochim. Cosmochim. Acta.*, 49, 1931-1941.
- Langmuir, D., 1978. Uranium solution mineral equilibria at low temperatures with application to sedimentary ore deposits. *Geochim. Cosmochim. Acta*, 42, 547-569.
- Langmuir, D. and Herman, J.S., 1980. The mobility of thorium in natural waters at low temperatures. *Geochim. Cosmochim. Acta.*, 44, 1753-1766.
- Mann, A.W., 1984. Mobility of gold and silver in lateritic weathering profiles: Some observations from Western Australia. *Econ. Geol.*, 79, 38-49.
- Rodgers, J.J.W. and Adams, J.A.S., 1974. Thorium. Abundance in rock forming minerals (I); thorium minerals (II); phase equilibria (III) and Uranium. Abundance in rock forming minerals (I), uranium minerals (II). in (Wedepohl, K.H. Ed.) *Handbook of Geochemistry* vol. II(5) Sections 90D and 92D. Springer-Verlag, Berlin.
- Scott, K.M., 1989a. Mineralogy and geochemistry of weathered shale profiles at the Panglo gold deposit, Eastern Goldfields, W.A., (AMIRA P241: Weathering Processes) CSIRO Division of Exploration Geoscience Restricted Report, 32R.
- Scott, K.M., 1989b. Mineralogy and geochemistry of weathered mafic/ultramafic volcanics from Section 4200N at Panglo, Eastern Goldfields, W.A., (AMIRA P241: Weathering Processes) CSIRO Division of Exploration Geoscience Restricted Report, 42R.
- Taylor, S.R. and McLennan, S.M., 1985. *The Continental Crust: its Composition and Evolution*. Blackwell Scientific Publications, Oxford.

Table 1: Radioelement results for Panglo drill hole profiles
(s.d = standard deviation)

Sample No	Depth (m)		K % s.d		eU ppm s.d		eTh ppm s.d		Identified Zones* (Scott 1988a, b)
PSRC 230 Mafic volcanics									
38317	0	1	0.60	0.10	1.71	0.43	1.4	1.1	calcite
38319	2	3	0.64	0.10	0.66	0.39	0.1	1.0	upper muscovite
38321	4	5	1.45	0.12	1.55	0.42	0.2	1.1	" "
38323	6	7	0.86	0.06	1.85	0.24	0.6	0.6	" "
38331	12	13	-0.04	0.09	0.65	0.37	0.1	1.0	kaol/goe
38335	16	17	0.06	0.09	0.44	0.36	-0.7	1.0	"
38339	20	21	2.23	0.13	0.22	0.39	1.5	1.1	lower muscovite
38341	22	23	0.68	0.06	0.52	0.22	0.8	0.6	" "
38347	28	29	0.01	0.09	0.17	0.35	0.0	1.0	kaol/goe/hem
38353	33	34	0.51	0.10	0.33	0.36	-0.4	1.0	"
38359	39	40	0.21	0.09	0.43	0.38	0.0	1.0	"
38361	41	42	0.02	0.05	0.22	0.21	-0.5	0.5	"
38363	43	44	0.06	0.09	0.65	0.39	0.1	1.0	"
38365	45	46	0.45	0.10	0.27	0.38	-0.5	1.0	musc / chlorite
38367	47	48	1.56	0.12	0.67	0.41	2.0	1.1	"
38371	51	52	0.97	0.11	0.44	0.39	-0.8	1.0	"
38381	60	61	1.71	0.12	0.44	0.39	-1.4	1.0	"
PSRC 231 Mafic volcanics									
38401	0	1	1.12	0.11	-0.16	0.37	-0.6	1.0	chlorite
38403	1	2	0.09	0.09	1.77	0.40	-0.5	1.0	"
38405	3	4	0.89	0.11	2.06	0.42	-0.9	1.1	"
38407	5	6	1.10	0.11	0.58	0.41	2.0	1.1	quartz poor
38415	13	14	1.30	0.11	0.11	0.38	-0.7	1.0	" "
38422	20	21	0.50	0.10	0.57	0.39	0.5	1.0	kaol/ goe/ hem
38436	31	32	0.62	0.10	0.57	0.38	-0.3	1.0	"
38437	32	33	0.71	0.10	0.47	0.39	1.1	1.0	"
38443	38	39	0.36	0.09	0.33	0.38	0.5	1.0	"
38445	40	41	1.03	0.11	0.36	0.39	0.9	1.0	musc/ kaol/ goe
38449	44	45	0.76	0.06	0.19	0.21	0.4	0.6	"
38457	51	52	1.03	0.11	0.58	0.40	0.7	1.1	"
38460	54	55	0.45	0.10	0.94	0.39	-0.7	1.0	"
38462	56	57	0.61	0.10	0.70	0.39	0.5	1.0	chlorite (low grade)
38466	60	61	0.07	0.05	0.19	0.21	0.6	0.5	" "
38468	62	63	0.23	0.09	0.56	0.38	-0.3	1.0	" "
38472	66	67	0.12	0.09	0.30	0.37	-0.3	1.0	chlorite
38474	68	69	0.48	0.10	-0.05	0.37	0.5	1.0	"
PSRCD 309 Unweathered rocks									
108070	129.3		0.00	0.08	0.03	0.41	1.1	0.9	mafic volc
108071	130.0		0.00	0.04	0.39	0.21	0.3	0.4	" "
108072	191.7		0.24	0.08	-0.13	0.41	0.0	0.8	dolerite
108073	192.4		0.26	0.08	0.02	0.41	0.1	0.9	"
PSRCD 232 Unweathered volcanics									
108064	136.5		0.03	0.04	0.94	0.21	0.0	0.4	mafic volc
PSRCD 306 Unweathred volcanics									
108066	128.5		1.35	0.10	0.04	0.43	0.2	0.9	mafic volc
108067	147.0		0.70	0.09	-0.09	0.41	0.4	0.9	" "

(Table 1 (cont'd)

Sample No	Depth (m)		%	K s.d	eU ppm	s.d	eTh ppm	s.d	Identified Zones* (Scott 1988a, b)
PSRCD 151 Dolerite intrusion									
22141	25.0		0.08	0.08	0.29	0.37	0.3	1.0	partially weathered
22143	27.0		0.03	0.09	0.04	0.37	0.6	1.0	" "
PSRC 340 Barren shale									
50352	0	1	0.76	0.06	2.29	0.26	7.2	0.8	alunite
50353	1	2	2.02	0.09	1.47	0.35	12.9	1.1	"
50355	3	4	2.17	0.12	1.38	0.44	10.9	1.2	"
50359	7	8	2.17	0.14	2.16	0.53	10.7	1.5	"
50365	13	14	2.02	0.14	1.57	0.51	10.3	1.4	paragonite
50377	24	25	1.77	0.13	2.07	0.52	10.4	1.4	"
50385	32	33	2.20	0.14	1.97	0.53	10.2	1.5	" (low grade)
50392	39	40	1.89	0.09	2.41	0.35	10.4	1.0	" "
50395	42	43	2.26	0.15	3.14	0.59	14.4	1.6	hematite
50406	52	53	2.12	0.13	1.76	0.50	7.8	1.4	"
50410	56	57	2.13	0.14	2.28	0.51	7.8	1.4	halite/ goe
50412	58	59	2.94	0.15	2.54	0.53	8.1	1.4	"
50413	59	60	1.93	0.14	2.81	0.52	6.5	1.4	"
PSRC 111 Mineralized Shale									
16421	0	1	1.65	0.12	1.05	0.45	2.9	1.3	alunite
16429	6	7	1.83	0.12	0.28	0.41	1.0	1.2	"
16437	14	15	3.83	0.15	0.38	0.47	3.5	1.4	"
16443	20	21	4.57	0.17	0.89	0.51	4.9	1.5	"
16449	26	27	2.44	0.13	1.43	0.47	4.0	1.4	"
16450	27	28	2.87	0.08	0.78	0.28	5.5	0.9	kaol/musc
16454	30	31	2.71	0.14	0.42	0.50	10.4	1.6	"
16457	33	34	2.04	0.13	2.10	0.52	7.4	1.5	"
16459	35	36	2.11	0.14	4.60	0.57	6.8	1.6	"
16460	36	37	2.16	0.13	2.04	0.46	8.3	1.3	"
16461	37	38	2.41	0.14	0.94	0.43	7.6	1.3	"
16463	39	40	1.63	0.12	0.77	0.40	3.5	1.2	" (min)
16464	40	41	1.74	0.12	0.87	0.40	4.6	1.2	" "
16467	43	44	1.31	0.06	0.72	0.20	3.7	0.6	" "
16471	47	48	1.80	0.12	0.48	0.38	3.6	1.1	kaol/musc
16473	49	50	2.04	0.13	0.97	0.43	7.6	1.3	"
16479	53	54	1.72	0.12	0.94	0.43	8.1	1.3	"
16481	55	56	1.70	0.12	1.63	0.42	3.5	1.2	"
16485	59	60	1.70	0.12	0.54	0.40	5.3	1.2	"
PSRC 341 Mineralized Shale									
50414	0	1	1.15	0.06	1.99	0.23	5.7	0.7	alunite
50415	1	2	2.54	0.13	0.99	0.41	3.8	1.2	"
50417	3	4	2.70	0.14	1.10	0.41	2.3	1.2	"
50428	12	13	2.62	0.15	2.34	0.49	11.3	1.5	"
50440	24	25	1.83	0.13	2.61	0.48	9.2	1.4	"
50443	27	28	2.14	0.13	1.33	0.43	6.9	1.3	kaol/musc
50449	33	34	1.21	0.06	1.03	0.21	5.6	0.7	"
50459	42	43	1.43	0.12	0.99	0.41	7.0	1.2	"
50460	43	44	2.09	0.13	1.27	0.43	7.2	1.3	paragonite
50462	45	46	1.86	0.13	0.75	0.43	8.0	1.3	"
50465	48	49	1.91	0.13	1.34	0.47	12.5	1.5	"
50470	53	54	1.56	0.13	2.66	0.50	14.7	1.5	"
50472	55	56	2.55	0.09	1.55	0.29	12.1	1.0	"
50474	57	58	2.43	0.14	1.58	0.47	10.1	1.4	kaol/musc
50477	59	60	1.99	0.13	1.87	0.46	9.1	1.4	"

(Table 1(cont'd)

Table 1 (Cont'd)									
Sample No	Depth (m)		K % s.d		eU ppm s.d		eTh ppm s.d		Identified Zones* (Scott 1988a, b)
PSRC 342 Mineralized Shale									
50478	0	1	2.62	0.14	1.44	0.43	2.6	1.2	kaolinite
50479	1	2	3.68	0.09	0.75	0.28	1.1	0.8	"
50481	3	4	2.93	0.14	1.15	0.44	1.1	1.2	"
50483	5	6	1.60	0.12	0.00	0.39	3.2	1.1	"
50485	7	8	1.35	0.12	1.12	0.43	3.4	1.1	alunite
50495	17	18	2.63	0.08	0.66	0.28	4.6	0.8	"
50501	23	24	1.14	0.11	2.00	0.45	3.9	1.2	"
50509	30	31	2.88	0.14	1.39	0.48	5.1	1.3	musc/kaol
50518	39	40	2.56	0.14	1.45	0.49	7.0	1.3	"
50519	40	41	1.46	0.12	2.67	0.47	8.5	1.4	" (min)
50520	41	42	1.88	0.14	3.24	0.56	11.2	1.5	" (min)
50521	42	43	2.32	0.14	1.85	0.49	11.5	1.5	"
50524	45	46	1.60	0.13	1.70	0.48	7.6	1.3	carbonate
50528	47	48	1.44	0.12	1.80	0.46	5.6	1.2	"
50534	53	54	1.43	0.12	0.90	0.43	3.3	1.2	paragonite
50538	57	58	1.19	0.11	1.50	0.44	3.5	1.1	" (min)
PSRCD 309 Unweathered shale									
105681	154.1		1.61	0.12	0.66	0.40	5.4	1.2	carb. shale
105682	173.1		3.08	0.08	0.88	0.24	4.8	0.8	" "
105683	222.1		1.22	0.11	1.51	0.41	4.0	1.2	dolomitic shale
PSRCD 310 Unweathered shale									
108074	217.0		3.01	0.09	1.25	0.29	5.3	0.9	dolomitic shale
108075	219.5		1.66	0.12	1.16	0.45	5.5	1.3	carb. shale
108076	174.0		1.12	0.06	0.81	0.22	2.7	0.7	dolomitic shale

 kaol = kaolinite; goe = goethite; musc = muscovite;
 hem = hematite; min = Au mineralization; volc = volcanic;
 carb = carbonaceous.

Table 2: Recount data for volcanics and shales, Panglo.
(s.d = standard deviation)

Sample No	K (%)			eU (ppm)			eTh (ppm)		
	(1)	(2)	s.d	(1)	(2)	s.d	(1)	(2)	s.d
a) Volcanics									
38371	0.97	0.95	0.11	0.44	0.09	0.39	-0.8	0.3	1.0
38422	0.50	0.62	0.10	0.57	0.13	0.38	0.5	0.7	1.1
38460	0.45	0.49	0.10	0.94	0.17	0.38	-0.7	0.5	1.0
38474	0.48	0.72	0.10	-0.05	-0.19	0.37	0.5	1.1	1.0
b) Shale									
50353	2.02	2.10	0.14	1.47	1.55	0.52	12.9	11.2	1.5
50406	2.12	2.15	0.13	1.76	1.62	0.50	7.8	7.4	1.4
50524	1.60	1.39	0.13	1.70	1.73	0.48	7.6	6.9	1.3

Table 3: Comparison of U and Th measured by delayed neutron counting and XRF respectively, with gamma-spectrometry derived eU and eTh for 13 samples of weathered shales from PSRC 340.

Sample No	Depth (m)		U ppm	eU ppm	s.d	U/eU	Th ppm	eTh ppm	s.d	Th/eTh
50353	1	2	1.88	1.47	0.35	1.28	14.0	12.9	1.1	1.1
50355	3	4	1.86	1.38	0.44	1.35	14.0	10.9	1.2	1.3
50359	7	8	1.74	2.16	0.53	0.81	14.0	10.6	1.5	1.3
50377	24	25	2.39	2.07	0.52	1.15	16.0	10.4	1.4	1.5
50385	32	33	1.99	1.97	0.53	1.01	12.0	10.2	1.5	1.2
50392	39	40	2.03	2.41	0.35	0.84	8.0	10.4	1.0	0.8
50395	42	43	2.58	3.14	0.59	0.82	16.0	14.4	1.6	1.1
50397	44	45	1.74	2.06	0.46	0.84	9.0	9.1	1.4	1.0
50401	48	49	1.83	1.09	0.26	1.68	10.0	9.5	0.9	1.1
50406	52	53	1.58	1.76	0.50	0.90		7.8	1.4	
50410	56	57	2.04	2.28	0.51	0.89	10.0	7.8	1.4	1.3
50412	58	59	2.17	2.54	0.53	0.85	12.0	8.1	1.4	1.5
50413	59	60	2.05	2.81	0.52	0.73	6.0	6.5	1.4	0.9

Table 4: Average abundances of radioelements in weathered shales from four drill holes, Panglo (derived from Table 1).

Hole No	K %		eU ppm		eTh ppm		eTh/eU	
	mean	s.d	mean	s.d	mean	s.d	mean	s.d
341	2.0	0.5	1.6	0.5	9.2	3.3	5.7	2.3
342	2.0	0.7	1.5	0.7	6.0	3.0	3.2	1.8
111	2.2	0.8	1.2	1.0	5.4	2.3	6.5	5.0
340	2.0	0.4	2.1	0.5	10.3	2.0	5.1	2.0

Table 5: Radioelement concentrations in soils at Panglo.

Sample No	North (m)	East (m)	K		eU		eTh		eTh/eU
			%	s.d	ppm	s.d	ppm	s.d	
108077	3900	2390	0.37	0.04	3.40	0.20	9.3	0.6	2.7
108078	4200	2775	0.86	0.05	2.28	0.23	6.0	0.7	2.6
108079	4200	2750	0.67	0.05	1.97	0.22	6.6	0.6	3.3
108080	4200	2730	0.71	0.05	1.76	0.21	5.7	0.6	3.2
108081	4200	2710	0.62	0.03	1.65	0.13	5.8	0.4	3.5
108082	4200	2690	0.77	0.05	1.96	0.21	6.4	0.6	3.3
108084	4200	2675	0.57	0.05	2.14	0.22	5.6	0.6	2.6
108086	4200	2660	0.69	0.05	2.05	0.22	5.9	0.6	2.9
108088	4200	2650	0.72	0.05	2.13	0.22	5.8	0.6	2.7
108089	4200	2645	0.60	0.05	1.51	0.20	5.6	0.6	3.7
108091	4200	2630	0.61	0.03	1.79	0.14	6.1	0.4	3.4
108093	4200	2616	0.75	0.05	1.60	0.21	5.9	0.6	3.7
108095	4200	2600	0.62	0.05	1.63	0.21	5.3	0.6	3.2
108097	4200	2587	0.42	0.04	1.91	0.20	4.8	0.6	2.5
108099	4200	2571	0.47	0.04	1.58	0.20	4.9	0.6	3.1
108100	4200	2560	0.41	0.05	2.14	0.25	6.1	0.7	2.8
108104	4200	2540	0.28	0.03	2.88	0.17	7.1	0.5	2.5
108106	4200	2520	0.74	0.05	1.93	0.22	6.0	0.6	3.1
108108	4200	2482	0.54	0.03	2.43	0.17	8.4	0.5	3.4
108109	4200	2460	0.45	0.04	1.37	0.20	4.9	0.6	3.6
108111	4200	2440	0.52	0.05	2.37	0.23	6.1	0.6	2.6
108112	4200	2420	0.57	0.06	2.59	0.27	6.9	0.7	2.7
108113	4200	2400	0.51	0.06	2.52	0.26	6.2	0.7	2.4
108115	4300	2420	0.76	0.05	2.19	0.23	6.7	0.7	3.1
108116	4300	2381	0.66	0.05	2.66	0.23	6.5	0.7	2.5
108117	4300	2300	0.33	0.05	3.06	0.29	8.5	0.8	2.8
108119	4300	2430	0.22	0.06	4.44	0.36	15.0	1.0	3.4

Table 6: Radioelement concentrations and Fe phases in pisoliths from soils at Panglo. Note: for sample 108102 C=coarse, F=finer, s=sinks, f=floats.

Sample No	North	East	K %	eU ppm	eTh ppm	He	Go	Mh*
108077	3900	2390	0.11	5.23	10.9	5		3
108102Cs	4200	2555	-0.08	4.86	7.7	5	4	3
108102Cf	4200	2555	0.02	2.81	4.5			
108102Fs	4200	2555	0.11	6.10	12.5	5	3	4
108102Ff	4200	2555	0.09	1.02	2.2	4		
108104	4200	2540	0.07	3.51	4.4	5	5	
108113	4200	2400	-0.04	4.94	8.3	5	3	2
108119	5000	2430	-0.04	4.96	17.1	5		3

*Abundances determined by X-ray diffractrometry

2 = minor, 3 = significant, 4 = moderate, 5 = abundant

He = hematite, Go = goethite, Mh = maghemite

Table 7: Selected chemical data from mineralized and barren holes through shale at Panglo.

Sample No	Depth (m)	K %	eU ppm	eTh ppm	Fe2O3 %	Ba ppm	Ca ppm	Sr ppm	Ce ppm	Au ppm
a) Barren hole PSRC 340										
50353	1- 2	2.02	1.47	12.9	2.63	750	680	130	75	0.010
50355	3- 4	2.17	1.38	10.9	2.19	660	680	160	29	0.010
50359	7- 8	2.17	2.16	10.7	2.62	450	300	200	48	0.010
50365	13-14	2.02	1.57	10.3	4.91	490	430	320	66	0.010
50377	24-25	1.77	2.07	10.4	3.42	540	370	260	42	0.001
50385	32-33	2.20	1.97	10.2	2.11	550	370	300	35	1.650
50392	39-40	1.89	2.41	10.4	6.20	560	210	190	27	0.750
50395	42-43	2.26	3.14	14.4	10.10	560	180	160	20	0.020
50397	44-45	1.82	2.06	9.1	9.46	530	200	140	1	0.050
50401	48-49	2.47	1.09	9.5	2.04	630	170	150	18	0.001
50406	52-53	2.12	1.76	7.8	-	-	-	-	-	0.030
50410	56-57	2.13	2.28	7.8	4.10	490	210	120	8	0.690
50412	58-59	2.94	2.54	8.1	5.36	590	200	120	11	0.900
50413	59-60	1.93	2.81	6.5	6.20	410	160	86	6	0.840
median		2.12	2.07	10.2	4.10	480	210	160	27	0.025
b) Mineralized hole PSRC 342										
50479	1- 2	3.68	0.75	1.1	2.67	530	340	33	9	0.010
50481	3- 4	2.93	1.15	1.1	12.40	420	360	46	39	0.010
50483	5- 6	1.60	0.00	3.2	14.50	250	340	29	38	0.020
50485	7- 8	1.35	1.12	3.4	18.10	220	210	46	55	0.020
50495	17-18	2.63	0.66	4.6	2.15	330	170	65	20	0.001
50501	23-24	1.14	2.00	3.9	5.96	210	92	32	37	0.001
50509	30-31	2.88	1.39	5.1	6.60	440	150	63	63	0.001
50518	39-40	2.56	1.45	7.0	3.35	500	190	92	56	0.001
50519	40-41	1.46	2.67	8.5	8.85	310	200	47	69	1.570
50520	41-42	1.88	3.24	11.2	10.80	440	260	42	80	2.700
50521	42-43	2.32	1.85	11.5	1.03	500	360	69	-	0.260
50524	45-46	1.60	1.70	7.6	6.52	290	2.73%	74	49	0.160
50528	47-48	1.44	1.80	5.6	6.75	280	3.50%	88	61	0.160
50534	53-54	1.43	0.90	3.3	3.66	240	390	71	11	0.010
50538	57-58	1.19	1.50	3.5	7.60	300	460	80	68	0.490
median		1.60	1.45	4.6	6.60	370	340	63	52	0.02
c) Unweathered shales										
105681	154	1.61	0.66	5.4	9.45	250	300	8	-	-
105683	173	1.22	1.51	4.0	2.65	270	8.03%	230	-	-
108074	217	3.01	1.25	5.3	1.34	550	0.64%	210	-	-
108075	219.5	1.66	1.16	5.5	5.35	320	2.17%	360	-	-
"average"		1.95	1.6	6.3	10.6	575	2.27%	180	42	-

Note "average" = average Australian Archaean shale (Taylor and McLennan, 1985, p181).

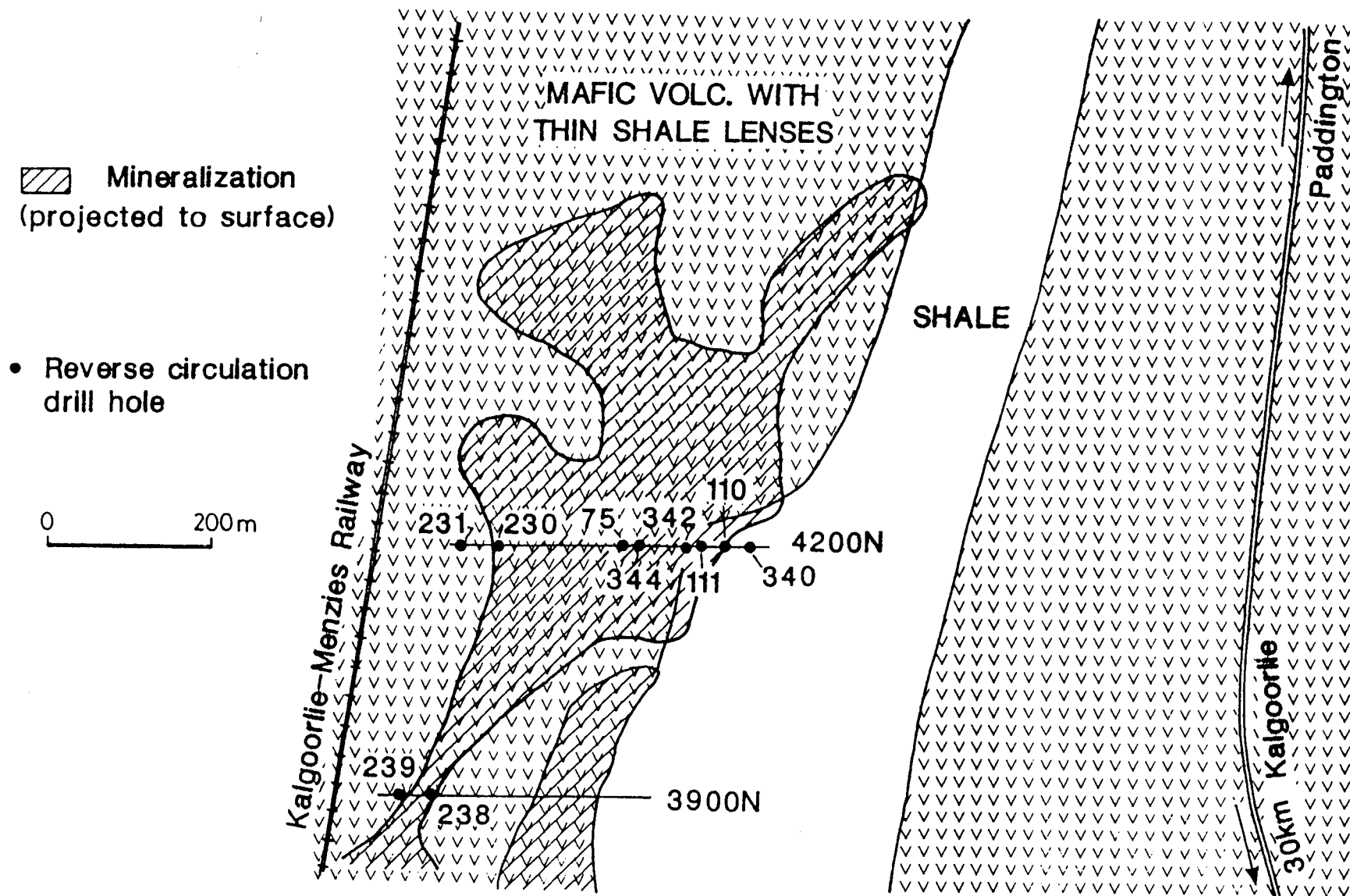


Fig 1: Location of reverse circulation drill holes sampled for this study (after mapping by Pancontinental Mining Ltd.)

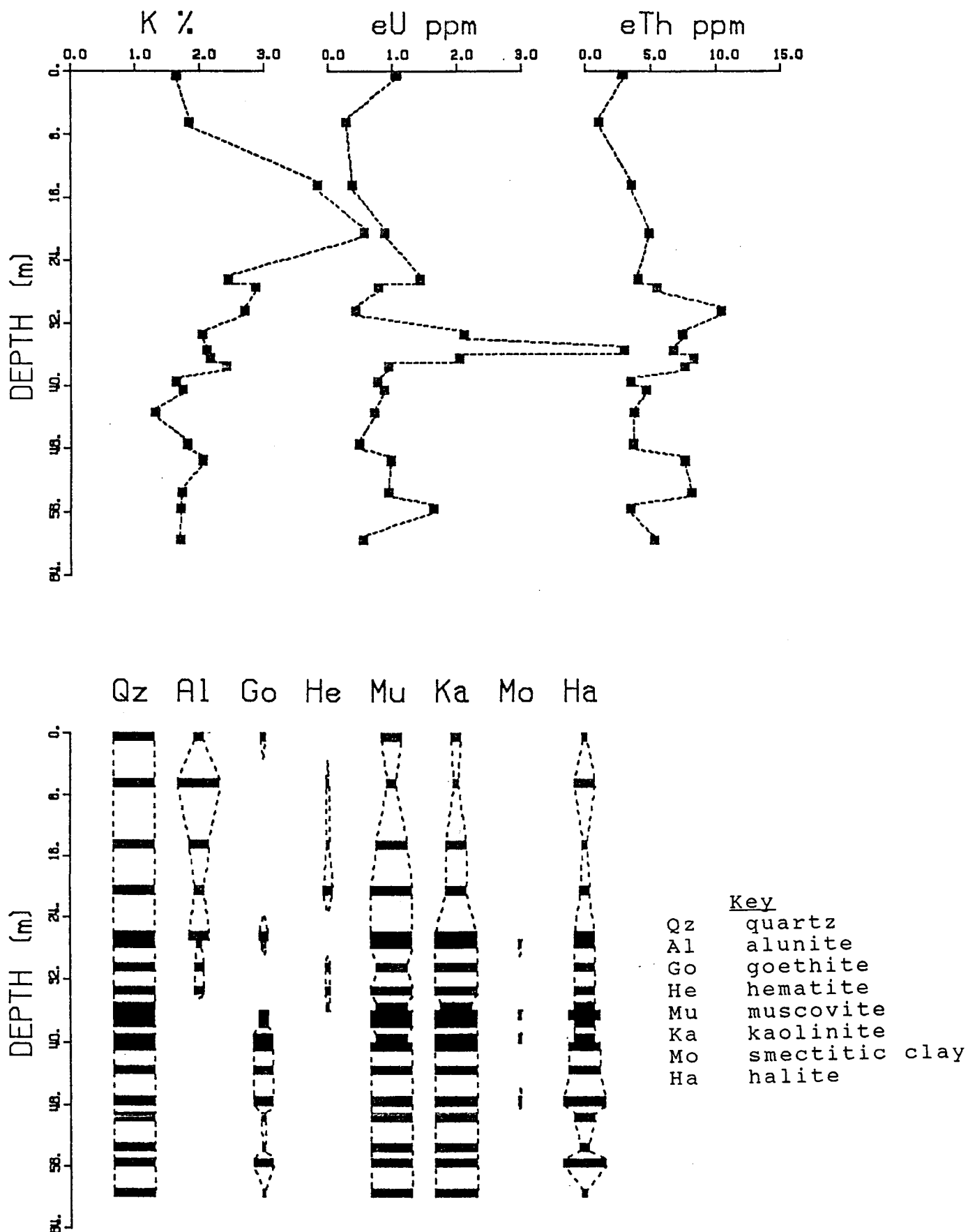


Fig 3: Mineralogical and radioelement profile through the mineralized hole PSRC 111.

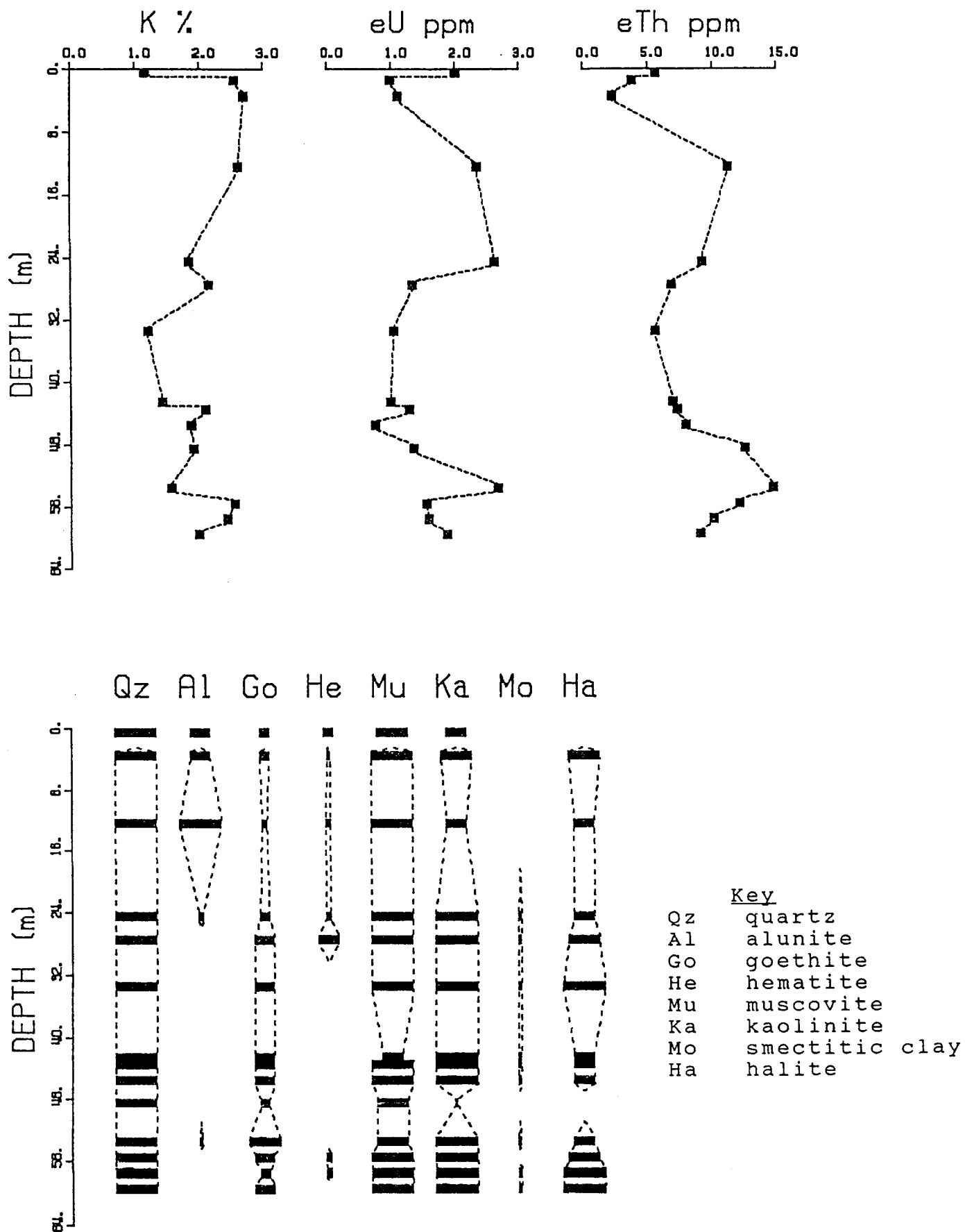


Fig 4: Mineralogical and radioelement profile through the mineralized hole PSRC 341.

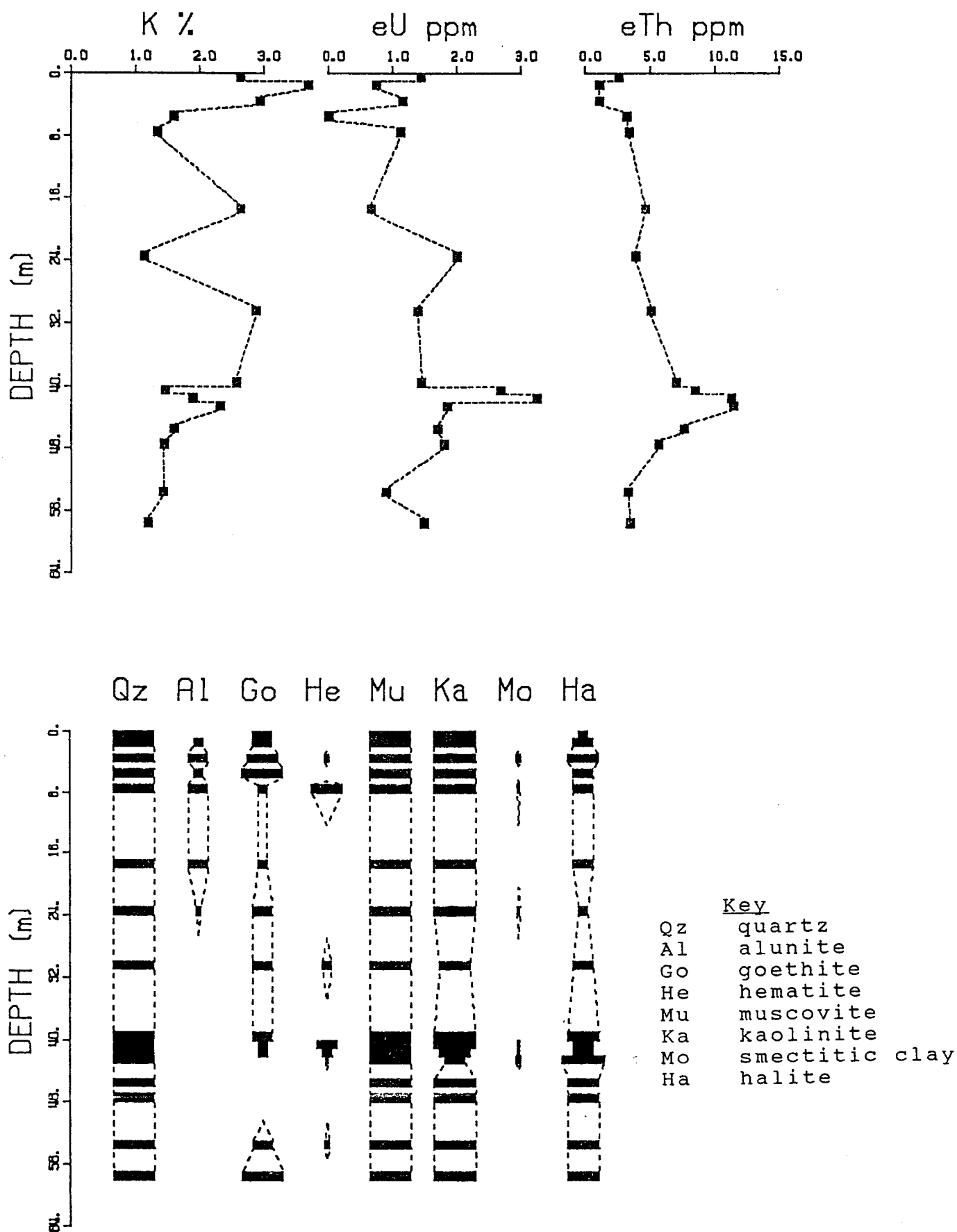


Fig 5: Mineralogical and radioelement profile through the mineralized hole PSRC 342.

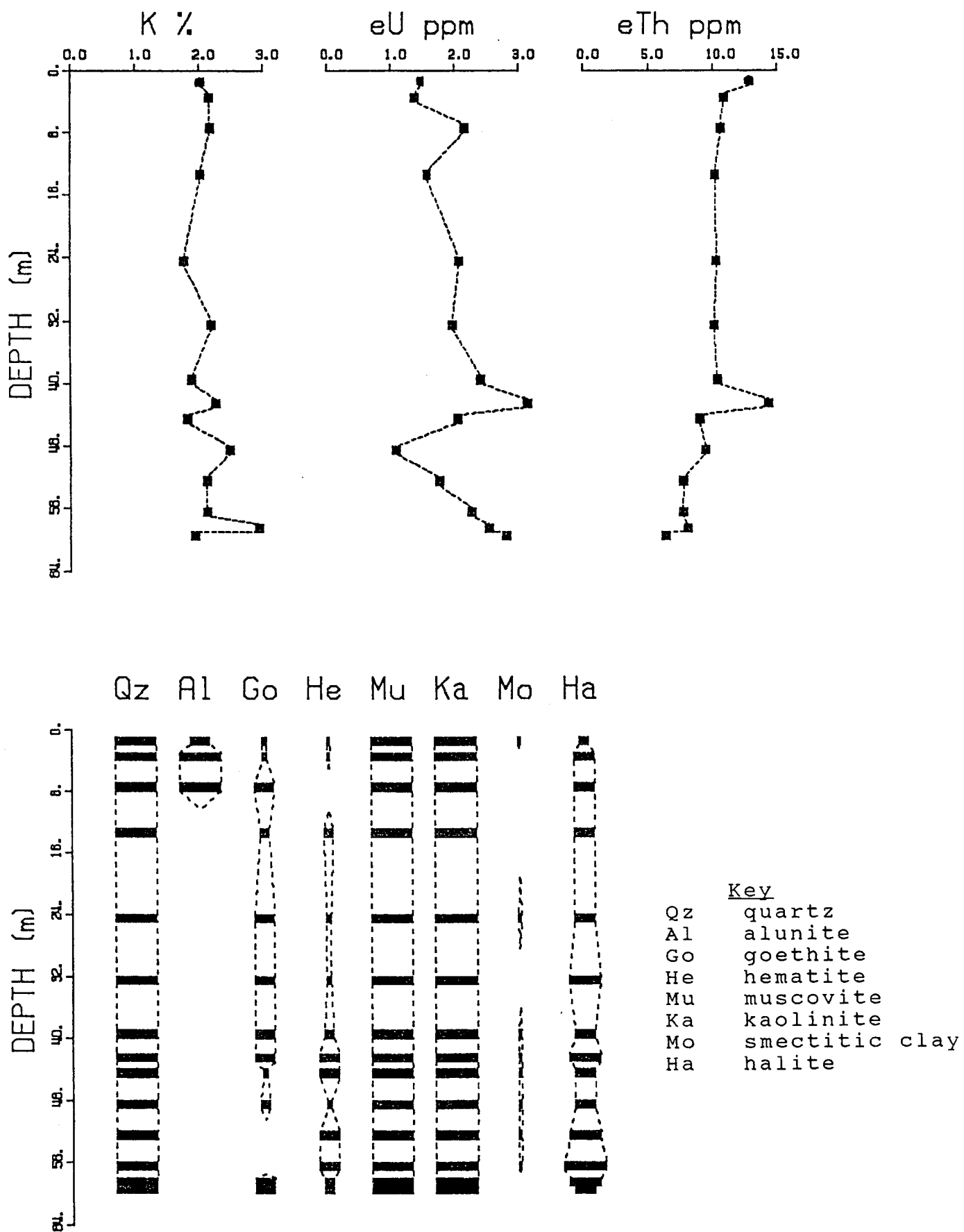


Fig 6: Mineralogical and radioelement profile through the barren hole PSRC 340.

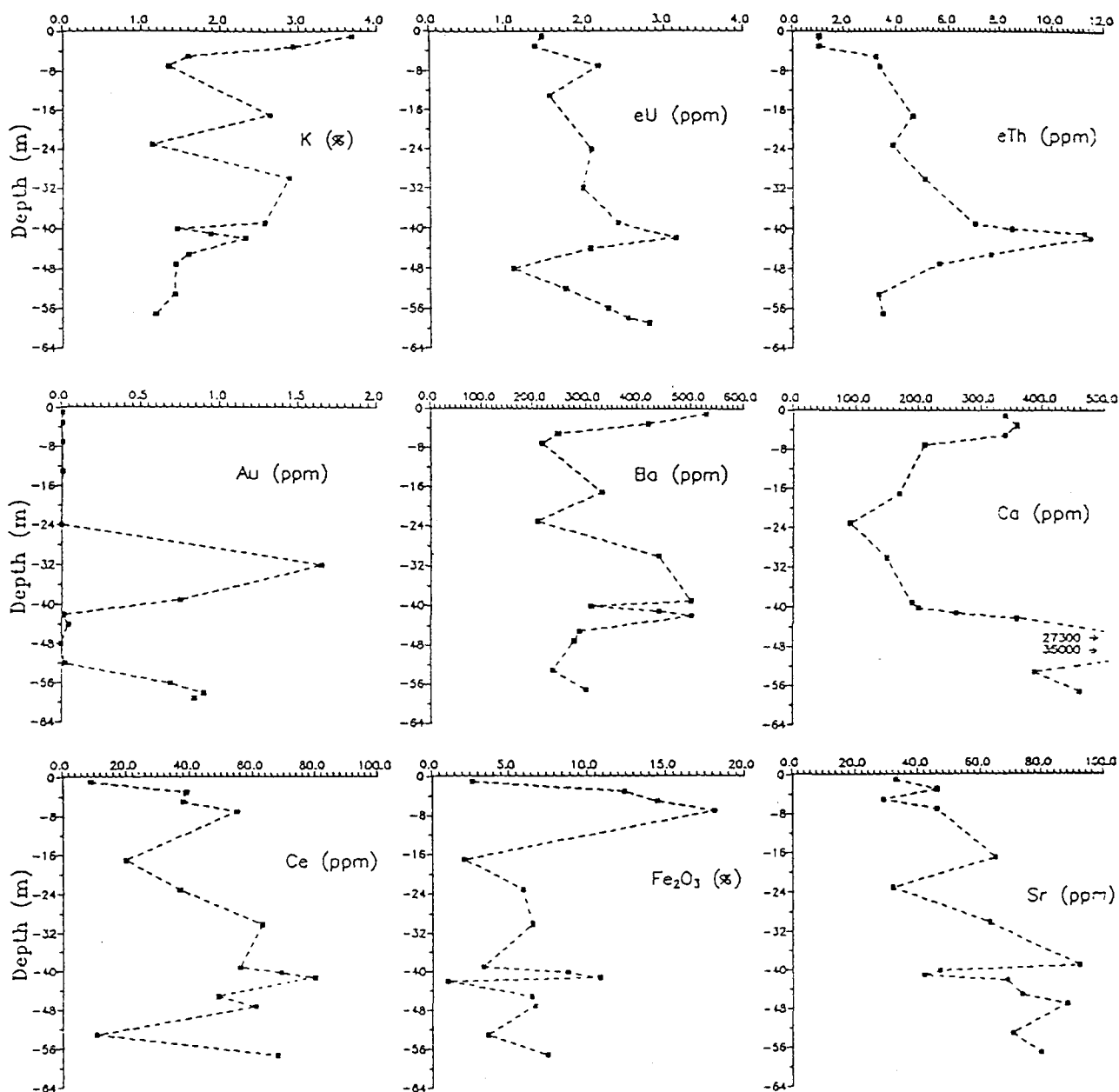


Fig 7: Profile of radioelements (K, eU and eTh) and the elements (Au, Ba, Ca, Ce, Fe and Sr) through the mineralized hole PSRC 342.

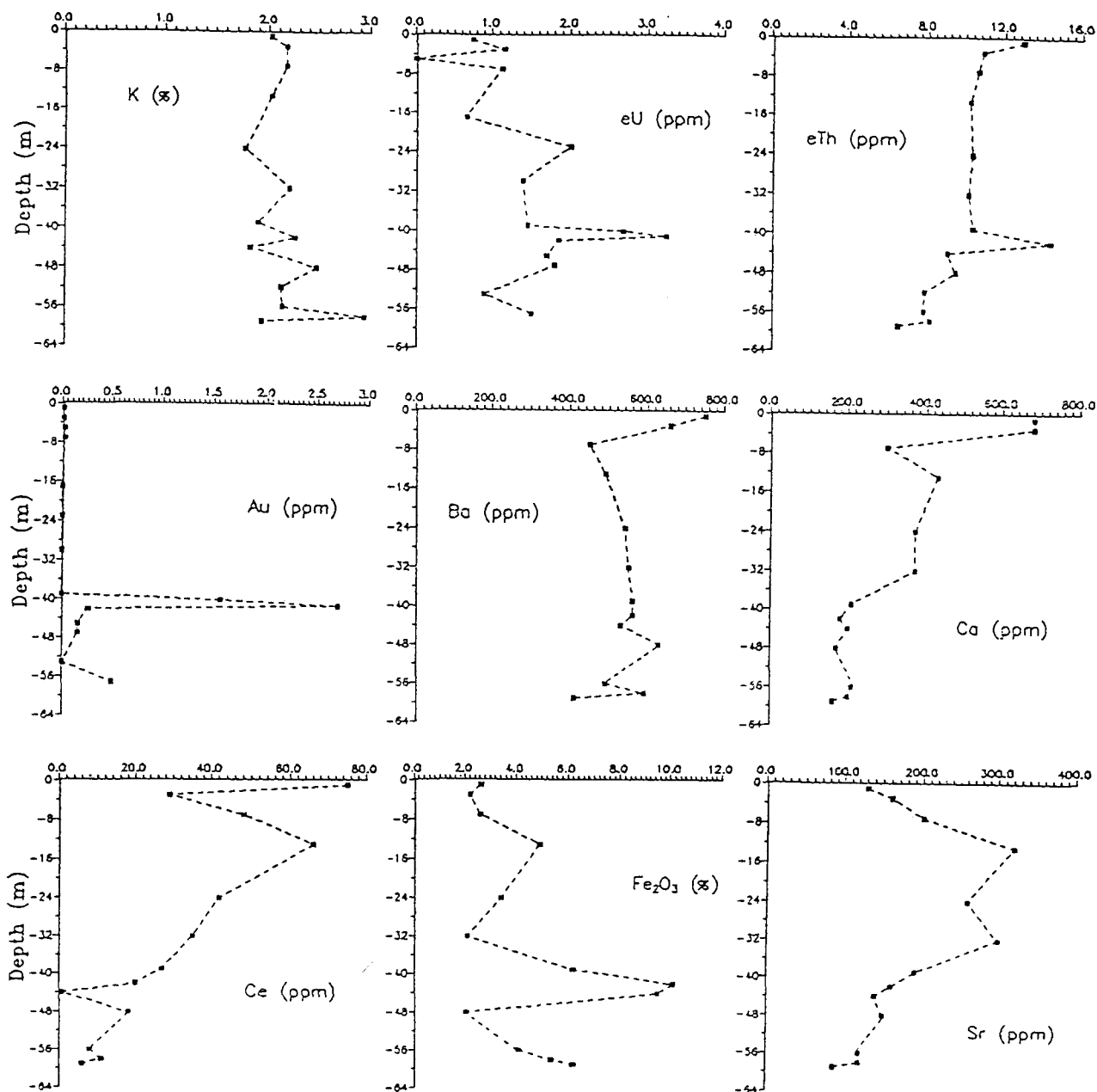


Fig 8: Profile of radioelements (K, eU and eTh) and the elements (Au, Ba, Ca, Ce, Fe and Sr) through the barren hole PSRC 340.